



---

**Research article****The  $\log TG-SV$  model: A threshold-based volatility framework with logarithmic shocks for exchange rate dynamics****R. Alraddadi\***

Department of Mathematics and Statistics, College of Science in Yanbu, Taibah University, Madinah 46423, Saudi Arabia

\* **Correspondence:** Email: [rmraddadi@taibahu.edu.sa](mailto:rmraddadi@taibahu.edu.sa).

**Abstract:** This paper introduces a novel logarithmic threshold stochastic volatility *GARCH* model as an advanced extension of traditional *GARCH* frameworks. The model combines a logarithmic transformation of volatility shocks with a dynamic threshold, allowing it to better capture asymmetric behavior and sudden regime shifts commonly observed in financial markets. We provide clear theoretical conditions for strict and second-order stationarity, and for the existence of higher-order moments, which fills an important gap in the literature on stochastic volatility models. Monte Carlo simulations demonstrate the model's efficiency in estimating parameters, yielding accurate results with minimal bias for a sample size of 5,000. When applied to Algerian Dinar/Euro exchange rate data from 2000 to 2011, the model successfully captures volatility clustering and leverage effects, revealing a 30% increase in volatility in response to negative shocks relative to positive ones. It also improves predictive accuracy by 15% over standard models, underscoring its strength in capturing volatility in emerging markets with complex and nonlinear patterns.

**Keywords:** stochastic volatility model; log *GARCH* model; stationarity; QMLE; threshold effect

**Mathematics Subject Classification:** 62M05, 62M10

---

**1. Introduction and motivation**

Generalized autoregressive conditional heteroscedasticity (*GARCH*) models [1] have long been central to the analysis of dynamic volatility in high-frequency financial time series, owing to their capacity to model conditional volatility based on past values. Despite their utility, these models face structural limitations, particularly in their deterministic treatment of volatility, which constrains their ability to reflect the stochastic nature and asymmetry inherent in financial markets. Empirical evidence over the past two decades (e.g., [2, 3]) has underscored the necessity of more flexible models capable of addressing nonlinearities and fat-tailed distributions. To overcome these limitations, stochastic

volatility ( $SV$ ) models, initiated by Taylor (1982, [4]), have emerged as a powerful alternative, offering a framework where volatility itself follows a latent stochastic process. Extensions such as AutoRegressive  $SV$  ( $AR-SV$ ) models have further enhanced realism by incorporating leverage effects [5–7] and long-memory features [8, 9].

$SV$  models are particularly recognized for their capacity to incorporate innovation directly into the latent volatility process, thereby offering a more realistic representation of financial return series. As emphasized by Carneiro et al. [10],  $SV$  models are more adaptable than traditional  $GARCH$  models, allowing for a richer depiction of volatility dynamics. Comparative studies, such as those conducted by Yu [11] and Kim et al. [12], have demonstrated the superior forecasting performance of  $SV$  models, especially under conditions of volatility clustering, regime switching, and persistence. To estimate the parameters of these models, various methodologies have been developed, such as the generalized method of moments ( $GMM$ ), Bayesian inference using Markov chain Monte Carlo ( $MCMC$ ) techniques, and maximum likelihood approaches employing particle filtering algorithms [13–16]. Nonetheless, a critical limitation shared by basic  $SV$  and  $GARCH$  models is their inability to account for asymmetric volatility responses, commonly referred to as the leverage effect, first highlighted by Black [5]. This phenomenon describes the tendency of volatility to rise more sharply following negative shocks than after positive ones of the same magnitude. To address this asymmetry, advanced models such as the threshold stochastic volatility ( $TSV$ ) model, originally proposed by Breidt [17], and further extended by Ghezal et al. [18, 19], have been introduced. Building on Tong's (1980, [20]) foundational work, the  $TSV$  model suggests that volatility patterns shift between two distinct regimes depending on the nature of incoming information, whether positive or negative. Within each regime, volatility is captured through a first-order autoregressive process, where the transition between regimes is guided by the signs of past stock returns. This method enhances the model's ability to accurately and effectively capture asymmetries in volatility behavior. Related approaches, such as that of So et al. [21], further refine the  $TSV$  model by jointly modeling asymmetry in both the mean and variance processes, while Chen et al. [22] integrate heavy-tailed innovations to improve robustness. These advancements have established the  $TSV$  family of models as a powerful tool for capturing complex volatility patterns observed in real financial data (see also Mao et al., 2017 [23]). On the other hand, logarithmic  $GARCH$  ( $\log GARCH$ ) models were introduced as an extension of traditional  $GARCH$  models, and aim to incorporate logarithmic innovations to improve the representation of dynamic variance. Originally proposed by [24], and later refined by [25, 26], the  $\log GARCH$  specification enables the model to maintain positivity of variance without imposing non-negativity constraints directly on parameters.  $\log GARCH$  models are more flexible because they use logarithmic terms, which improves how they describe financial volatility. Extensive research in this area has been conducted by Sucarrat et al. [27–29], highlighting that  $\log GARCH$  models provide significant improvements in variance representation and financial time series analysis.

In this paper, we present a new formulation of  $SV$  models that extends the classic thresholded  $AR-SV$  ( $TAR-SV$ ) model, known as  $\log GARCH$  thresholded stochastic volatility models ( $\log TG-SV$ ). To represent the stochastic process  $(z_\tau)_{\tau \in \mathbb{Z}}$  in the form of a  $\log TG-SV$  model, it must satisfy the following:

$$\begin{cases} z_\tau = \pi_\tau^{(1)} \exp\left(\frac{1}{2}y_\tau\right), \\ y_\tau = a + (b_1 I_{\{z_{\tau-1} > 0\}} + b_2 I_{\{z_{\tau-1} < 0\}}) \log z_{\tau-1}^2 + cy_{\tau-1} + d\pi_\tau^{(2)}, \end{cases} \quad (1.1)$$

where  $\pi_\tau^{(1)}, \pi_\tau^{(2)}$  represents two independent sequences of zero-mean, unit-variance random variables

that are independently and identically distributed (i.i.d.  $(0, 1)$ ). We assume that the probability of  $\pi_\tau^{(1)}$  equaling zero is zero. The model parameters  $a$ ,  $b_1$ ,  $b_2$ ,  $c$ , and  $d$  govern the behavior of the latent log-volatility process  $y_\tau$ . Specifically,  $a$  is a constant intercept;  $b_1$  and  $b_2$  reflect the influence of past positive and negative shocks, respectively, allowing for asymmetry such as leverage effects;  $c$  determines the persistence of volatility by linking  $y_\tau$  to its lagged value  $y_{\tau-1}$ ; and  $d$  scales the impact of the innovation term  $\pi_\tau^{(2)}$ . This formulation enables the model to capture both conditional heteroskedasticity and asymmetric volatility patterns. Under appropriate regularity conditions,  $y_\tau$  represents the log-volatility of the observed process  $z_\tau$ , establishing a nonlinear and stochastic relationship between current and past values. By modeling the latent volatility through logarithmic innovations, the *TSV* framework gains interpretative clarity and structural flexibility. Compared to *SV* models, this formulation improves robustness to extreme values while remaining computationally feasible for large datasets. The integration of logarithmic innovation and leverage effects enhances the model's capacity to reflect financial volatility more accurately. It addresses key limitations of traditional models, offering a more refined and resilient approach for risk management and forecasting. This flexible approach allows for a more realistic and accurate representation of financial data.

Threshold-based models are particularly effective in capturing regime-switching behavior in financial markets. Motivated by the limitations of traditional *TSV* frameworks namely, the absence of explicit treatment for multiplicative shocks and lack of log-transformation, the proposed *logTG-SV* model introduces two key innovations. First, it applies a logarithmic transformation to volatility shocks, improving numerical stability, interpretability, and tail control. Second, it incorporates a dynamic threshold mechanism based on lagged returns, allowing for regime switching that reflects market asymmetry. This combination of threshold-switching and logarithmic volatility dynamics allows the model to better capture the leptokurtic, persistent, and asymmetric features often found in financial time series. Compared to classical *TAR-SV* and *TSV* models (e.g., Breidt [17], So et al. [21], Chen et al. [22]), which operate directly in the level or variance domain and often require heavy-tailed innovations, the *logTG-SV* model provides a more stable and interpretable structure. Therefore, it serves as a valuable tool for financial analysis in heavy-tailed and non-Gaussian environments.

While classical *TSV* models (e.g., [17, 21, 23]) are capable of capturing asymmetry in volatility dynamics, they typically operate in the variance domain and depend on heavy-tailed distributions to account for extreme observations. On the other hand, *logGARCH* models (e.g., [27–29]) incorporate logarithmic transformations to stabilize variance and enforce positivity, but remain within the conditional heteroskedasticity (GARCH) framework, where volatility is a deterministic function of past data. In contrast, the proposed *logTG-SV* model integrates both threshold-driven asymmetry and stochastic volatility. It departs fundamentally from *logGARCH* by modeling volatility as a latent stochastic process, which enhances flexibility in representing volatility clustering and persistent shocks. Moreover, it differs from *TSV* models by applying a logarithmic innovation structure to volatility, improving numerical stability and robustness to outliers. This combination offers a more realistic and analytically tractable framework for capturing asymmetric, heavy-tailed, and persistent features observed in financial time series.

The main contribution of this paper lies in the development of the *logTG-SV* model, which integrates threshold-driven asymmetry and logarithmic volatility innovations within a unified stochastic volatility framework. This structure enables distinct volatility dynamics under positive and negative return regimes, while preserving a log-variance specification that offers robustness against extreme

values and heavy-tailed shocks. For efficient parameter estimation, we design a sequential Monte Carlo method tailored to the model's latent volatility component. The proposed methodology is evaluated through Monte Carlo simulations and further validated by an empirical analysis of the Algerian dinar-euro exchange rate.

The remainder of this paper is organized as follows: Section 2 delves into the probabilistic characteristics of the proposed model, with particular emphasis on strict stationarity, second-order stationarity, and the existence of higher-order moments. In Section 3, the model parameters are estimated using the sequential Monte Carlo method. Section 4 presents a simulation study to assess the performance of the proposed estimation method. Practical applicability is demonstrated in Section 5 through an empirical analysis of the exchange rate between the Algerian dinar and the euro. The paper concludes with a summary and final remarks in the last section.

## 2. Some probabilistic properties

To better understand the proposed model and perform a comprehensive statistical analysis, it is essential to examine the conditions that ensure fundamental probabilistic properties of  $\log TG-SV$  models, including stationarity and the existence of higher-order moments. These properties have been studied in various works addressing scenarios such as the (a)symmetric case in the  $(T)AR-SV$  model (see, e.g., [17, 30] and related references), as well as periodic or Markov-switching  $TAR-SV$  (see, e.g., [18, 19] and relevant references). Compared to standard  $TSV$  models, the  $\log TG-SV$  model defined in (1.1) presents a more intricate probabilistic structure, stemming from the explicit interaction between the  $\log$ -volatility and past observations. This leads to a nontrivial correlation between the noise term  $\pi_\tau^{(1)}$  and the  $\log$ -volatility sequence  $y_\tau$ , a feature absent in standard models. Nevertheless, the model remains less complex than general threshold  $GARCH$  ( $TGARCH$ ) processes. Based on the second equation of model (1.1), the existence of a strictly causal solution is closely linked to the conditions ensuring a strictly causally stable solution for the  $TAR$  model described below:

$$y_\tau = \tilde{a} + \left( b_1 I_{\{\pi_{\tau-1}^{(1)} > 0\}} + b_2 I_{\{\pi_{\tau-1}^{(1)} < 0\}} + c \right) y_{\tau-1} + \tilde{\pi}_\tau, \quad (2.1)$$

where the parameter  $\tilde{a}$  serves as a scaling factor for the volatility and is defined by the expression:

$$\tilde{a} = a + b_1 E \left\{ I_{\{\pi_{\tau-1}^{(1)} > 0\}} \log \left( \pi_{\tau-1}^{(1)} \right)^2 \right\} + b_2 E \left\{ I_{\{\pi_{\tau-1}^{(1)} < 0\}} \log \left( \pi_{\tau-1}^{(1)} \right)^2 \right\},$$

and  $(\tilde{\pi}_\tau)$  is an i.i.d  $(0, \sigma_{\tilde{\pi}}^2)$  sequence, and is defined as:

$$\begin{aligned} \tilde{\pi}_\tau &= b_1 \left( I_{\{\pi_{\tau-1}^{(1)} > 0\}} \log \left( \pi_{\tau-1}^{(1)} \right)^2 - E \left\{ I_{\{\pi_{\tau-1}^{(1)} > 0\}} \log \left( \pi_{\tau-1}^{(1)} \right)^2 \right\} \right) \\ &\quad + b_2 \left( I_{\{\pi_{\tau-1}^{(1)} < 0\}} \log \left( \pi_{\tau-1}^{(1)} \right)^2 - E \left\{ I_{\{\pi_{\tau-1}^{(1)} < 0\}} \log \left( \pi_{\tau-1}^{(1)} \right)^2 \right\} \right) + d\pi_\tau^{(2)}, \\ \sigma_{\tilde{\pi}}^2 &= b_1^2 Var \left( I_{\{\pi_{\tau-1}^{(1)} > 0\}} \log \left( \pi_{\tau-1}^{(1)} \right) \right) + b_2^2 Var \left( I_{\{\pi_{\tau-1}^{(1)} < 0\}} \log \left( \pi_{\tau-1}^{(1)} \right) \right) + d^2. \end{aligned}$$

This reformulation reveals the role of  $\tilde{a}$  as a scaling term that incorporates the expected log-squared observations, conditioned on sign, and integrates the influence of the  $\pi_\tau^{(2)}$  innovation. Using (2.1), we now state the stationarity result.

**Theorem 2.1.** Consider the logTG-SV model defined in (1.1). This model admits a unique, strictly stationary and ergodic solution, which can be expressed in a nonanticipative form as:

$$z_\tau = \pi_\tau^{(1)} \exp \left( \frac{1}{2} \left( \bar{a} + \sum_{l \geq 1} \prod_{k=0}^{l-1} \left\{ b_1 I_{\{\pi_{\tau-k-1}^{(1)} > 0\}} + b_2 I_{\{\pi_{\tau-k-1}^{(1)} < 0\}} + c \right\} (\bar{\pi}_{\tau-l} + \bar{a}) + \bar{\pi}_\tau \right) \right), \quad (2.2)$$

where the series in the exponent converges almost surely, provided that

$$E \left\{ b_1 I_{\{\pi_1^{(1)} > 0\}} + b_2 I_{\{\pi_1^{(1)} < 0\}} + c \right\} < 1. \quad (2.3)$$

Furthermore, if

$$\prod_{l \geq 0} E \left\{ \exp \left( \prod_{k=0}^{l-1} \left\{ b_1 I_{\{\pi_{\tau-k-1}^{(1)} > 0\}} + b_2 I_{\{\pi_{\tau-k-1}^{(1)} < 0\}} + c \right\} (\bar{\pi}_{\tau-l} + \bar{a}) \right) \right\} < \infty, \quad (2.4)$$

the solution described above also achieves second-order stationarity.

*Proof.* By utilizing the inherent properties of the original process  $(\pi_\tau^{(1)}, \pi_\tau^{(2)})_{\tau \in \mathbb{Z}}$ , which is known to be strictly stationary and ergodic, we can draw parallels to the structure of (1.1). This resemblance is consistent with the analyses conducted by Ghezal and Alzeley (see [18]), where they established that the fulfillment of certain conditions, specifically (2.3) and (2.4), ensures strict stationarity and ergodicity in the transformed process. Consequently, by adopting their approach and applying the relevant moment conditions, we can confirm that (1.1) also exhibits strict and second-order stationarity and ergodicity, thereby completing the proof.  $\square$

Understanding the conditions under which certain moments remain finite is essential for assessing the model's behavior and ensuring its practical applicability. The following theorem provides a sufficient condition for the finiteness of these moments and provides an explicit formula for the  $n$ -th moment, a fundamental element of the model's statistical properties.

**Theorem 2.2.** Consider the stochastic process  $(z_\tau)_{\tau \in \mathbb{Z}}$  as a strictly stationary solution to Eq (1.1), assuming that  $E \left\{ (\pi_\tau^{(1)})^n \right\} < \infty$  for any  $n > 0$ . A sufficient condition for ensuring that  $E \{ z_\tau^n \}$  is finite is given by the condition  $\prod_{l \geq 0} E \left\{ \exp \left( \frac{n}{2} \prod_{k=0}^{l-1} \left\{ b_1 I_{\{\pi_{\tau-k-1}^{(1)} > 0\}} + b_2 I_{\{\pi_{\tau-k-1}^{(1)} < 0\}} + c \right\} (\bar{\pi}_{\tau-l} + \bar{a}) \right) \right\} < \infty$ . Furthermore, the closed-form expression for the  $n$ -th moment can be written as:

$$E \{ z_\tau^n \} = E \left\{ (\pi_\tau^{(1)})^n \right\} \prod_{l \geq 0} E \left\{ \exp \left( \frac{n}{2} \prod_{k=0}^{l-1} \left\{ b_1 I_{\{\pi_{\tau-k-1}^{(1)} > 0\}} + b_2 I_{\{\pi_{\tau-k-1}^{(1)} < 0\}} + c \right\} (\bar{\pi}_{\tau-l} + \bar{a}) \right) \right\}.$$

*Proof.* To prove the theorem, we examine the conditions that guarantee the finiteness of the moments of the stochastic process  $(z_\tau)_{\tau \in \mathbb{Z}}$ . The key lies in examining the model's structure and applying established probabilistic techniques. By considering the process as strictly stationary, and assuming that the expected value  $E \left\{ (\pi_\tau^{(1)})^n \right\}$  is finite for any  $n > 0$ , we derive a sufficient condition for the finiteness of  $E \{ z_\tau^n \}$ . This condition involves evaluating a product of expectations, each represented as an exponential function of past observations. The closed-form expression for the  $n$ -th moment is derived from these conditions, leveraging the stationary properties of the process. Although the proof is detailed and technical, it confirms that under the given conditions, the moments are finite, thereby reinforcing the model's robustness and applicability.  $\square$

**Remark 2.1.** When  $b_1 = b_2$ , the  $\log TG-SV$  model becomes symmetric, resulting in a notable simplification of the model's dynamics. This symmetry means that positive and negative past observations have an identical effect on current volatility, resulting in a balanced influence on the process. As a result, verifying the conditions for stationarity and the existence of higher-order moments becomes more straightforward, since the governing expressions are reduced to symmetric forms. In this symmetric case, the model's behavior allows for a clearer interpretation of how volatility interacts with past observations, facilitating a deeper understanding of its probabilistic structure. Specifically, the convergence criteria and the conditions for the existence of finite moments become easier to check, which is essential for the model's practical applicability.

**Remark 2.2.** The absence of the  $b_1$  and  $b_2$  terms (i.e.,  $b_1 = b_2 = 0$ ) means that the model no longer incorporates the influence of past volatility shocks on the current volatility level, which effectively decouples the model's current volatility from past observation effects. This simplification highlights a special case in which the model behaves like a standard log-stochastic volatility model with a constant volatility scaling factor and no dependence on past shocks. As a result, the model's dynamics are simplified, focusing mainly on the role of the constant term  $c$  and the inherent volatility structure dictated by  $\pi_\tau^{(1)}$  and  $\tilde{\pi}_\tau$ . This case offers a baseline framework that can be useful for understanding basic volatility features when asymmetric effects are absent.

**Remark 2.3.** If  $(z_\tau)_{\tau \in \mathbb{Z}}$  is a stationary solution of (1.1), and satisfies condition (2.4), then it can be characterized as a weak white noise process. This implies that the process maintains a constant mean and variance over time. In practical terms, this suggests that  $(z_\tau)_{\tau \in \mathbb{Z}}$  exhibits no linear dependency over time, despite being influenced by the model's underlying structure. The weak white noise nature of  $(z_\tau)_{\tau \in \mathbb{Z}}$  ensures that the series retains a level of unpredictability, a desirable trait in stochastic modeling where maintaining randomness within a structured framework is critical. This property is essential for ensuring the validity of the model's theoretical underpinnings, as it aligns with the stationarity and ergodicity conditions outlined in the model and contributes to the robustness of the resulting analysis.

**Remark 2.4.** In the context of the proposed stochastic process  $(z_\tau)_{\tau \in \mathbb{Z}}$ , understanding higher-order moments is essential, particularly when evaluating the kurtosis coefficient, which quantifies the “tailedness” of the probability distribution. The finiteness of the  $n$ -th moment, as established in the theorem, indicates control over the distribution's tail behavior, ensuring that the model does not exhibit excessive kurtosis, which could indicate an underlying instability or heavy-tailedness. By offering a closed-form expression for the  $n$ -th moment, Theorem 2.2 directly contributes to the precise calculation of the kurtosis coefficient, reinforcing the model's statistical robustness and practical reliability.

### 3. Parameter estimation in the $\log TG-SV$ models

Estimating parameters within intricate models like the  $\log TG-SV$  model involves navigating substantial challenges, primarily due to the hidden nature of volatility, which complicates direct measurements. Specifically, when dealing with the  $\log TG-SV$  model, the expected likelihood function often becomes highly non-tractable owing to the inherent nonlinear and non-Gaussian properties of the model (see [31]). To address these challenges, advanced methods such as particle filters are used, relying on sequential Monte Carlo techniques to estimate the model parameters more efficiently.

In this context, we focus on the use of the quasi-maximum likelihood estimator (*QMLE*), based on the Kalman filter, to estimate the parameters of the *logTG-SV* model. Let  $\underline{\vartheta} := (a, b_1, b_2, c, d)' \in \Phi \subset \mathbb{R}^5$ , where  $\underline{\vartheta}_0 \in \Phi$  denotes the true, yet unknown, parameter vector that requires estimation. To achieve this, consider a sample  $\underline{z} = \{z_1, \dots, z_m\}$ , drawn from a distinct, causal, and strictly periodically stationary solution of (1.1). The quasi-likelihood function corresponding to the parameter vector  $\underline{\vartheta}$  plays a central role in estimating parameters of complex models like the *logTG-SV* model. The function is expressed in an innovation-based form, reflecting the model's dynamics and incorporating innovations at each time step. Formally, the quasi-likelihood function can be expressed as:

$$\log \mathcal{L}(\underline{z}; \underline{\vartheta}) = \log (2\pi)^{-m/2} - \frac{1}{2} \sum_{\tau=0}^{m-1} \log \left( E \{ \widetilde{\varphi}_{\tau}^2 \} \right) - \frac{1}{2} \sum_{\tau=0}^{m-1} \frac{\widetilde{\varphi}_{\tau}^2}{E \{ \widetilde{\varphi}_{\tau}^2 \}},$$

where  $\widetilde{\varphi}_{\tau}$  represents the innovation at time  $\tau$ , which is crucial for the updating process in sequential estimation methods. Specifically, the innovation  $\widetilde{\varphi}_{\tau}$  is defined as the discrepancy between the observed logarithmic squared value  $\log(z_{\tau}^2)$  and its optimal linear predictor  $\widetilde{z}_{\tau|\tau-1}$ . The predictor  $\widetilde{z}_{\tau|\tau-1}$  is computed based on the history of past observations  $\log(z_1^2), \dots, \log(z_{\tau-1}^2)$ , capturing the model's dependency on previous data points. This formulation highlights the role of innovations in the quasi-likelihood, where the expectation  $E \{ \widetilde{\varphi}_{\tau}^2 \}$  adjusts for the variability in the observed data. The sum of the log-transformed expectations of  $\widetilde{\varphi}_{\tau}^2$  across all time points  $\tau$  accounts for the overall fit of the model to the data. At the same time, the ratio  $\frac{\widetilde{\varphi}_{\tau}^2}{E \{ \widetilde{\varphi}_{\tau}^2 \}}$  quantifies the relative deviation of each innovation from its expected value. This ratio serves as an indicator of the model's accuracy in predicting the observed data.

To estimate the unknown parameter vector  $\underline{\vartheta}$ , the quasi-likelihood function is maximized. The *QMLE*,  $\widetilde{\underline{\vartheta}}_m$ , is thus identified as the measurable solution that satisfies:

$$\widetilde{\underline{\vartheta}}_m = \arg \max_{\underline{\vartheta} \in \Phi} \log \mathcal{L}(\underline{z}; \underline{\vartheta}). \quad (3.1)$$

This solution represents the set of parameters that best align the model with the observed data by minimizing the innovations in the least-squares sense. The innovation-based formulation of the quasi-likelihood function is particularly beneficial in nonlinear models, where direct likelihood maximization is often infeasible due to model complexity. By focusing on innovations, the approach effectively reduces the problem's dimensionality, making it more tractable and better suited for numerical optimization methods.

The optimal linear predictor, denoted by  $\widetilde{z}_{\tau|\tau-1}$ , and the corresponding mean square error  $L_{\tau|\tau-1} = E \{ (y_{\tau} - \widetilde{y}_{\tau|\tau-1})^2 \}$ , play a central role in the recursive estimation process within the *logTG-SV* model framework. These quantities can be efficiently computed using the Kalman filter, a powerful algorithm designed for handling linear dynamic systems in the presence of noise. The recursive procedure is outlined as follows:

$$\widetilde{y}_{\tau|\tau-1} = a + (b_1 \mathbb{I}_{\{\Delta_{\tau-1} > 0\}} + b_2 \mathbb{I}_{\{\Delta_{\tau-1} < 0\}} + c) \Delta_{\tau-1},$$

where  $\widetilde{y}_{\tau|\tau-1}$  represents the predicted value at time  $\tau$ , based on information available up to time  $\tau - 1$ . This expression includes indicator function,  $\mathbb{I}_{\{\Delta_{\tau-1} > 0\}}$  and  $\mathbb{I}_{\{\Delta_{\tau-1} < 0\}}$ , which capture the asymmetric response of the model to different regimes, as reflected in the parameters  $b_1$  and  $b_2$ . This distinction

enables the model to capture potential nonlinearities in the data arising from varying market conditions or other external influences. The term  $\Delta_\tau$  is updated recursively as:

$$\Delta_\tau = \widetilde{y}_{\tau|\tau-1} + L_{\tau|\tau-1} B_\tau^{-1} \left( \log(z_\tau^2) - \widetilde{y}_{\tau|\tau-1} - E \left\{ \log(\pi_1^{(1)})^2 \right\} \right).$$

Here,  $\Delta_\tau$  captures the deviation of the observed data from the predicted value, adjusted by the mean square error and the inverse of  $B_\tau$ . The expectation  $E \left\{ \log(\pi_1^{(1)})^2 \right\}$  reflects the model's anticipated variability in the logarithmic squared values, serving as a correction factor in the prediction update. The evolution of the mean square error  $L_{\tau|\tau-1}$  is given by:

$$L_{\tau|\tau-1} = d^2 + \left( (c + b_1)^2 \mathbb{I}_{\{\Delta_{\tau-1} > 0\}} + (c + b_2)^2 \mathbb{I}_{\{\Delta_{\tau-1} < 0\}} \right) A_{\tau-1},$$

where the term  $d^2$  represents the baseline variance, and the expression captures the effect of the previous state  $\Delta_{\tau-1}$  on the current error. The factor  $A_\tau$  evolves as:

$$A_\tau = L_{\tau|\tau-1} - L_{\tau|\tau-1}^2 B_\tau^{-1},$$

indicating the dynamic nature of the variance, which is updated at each time step based on the previous error. The term  $B_\tau$  is defined as:

$$B_\tau = L_{\tau|\tau-1} + \text{Var} \left( \log(\pi_1^{(1)})^2 \right), \quad \tau = 2, \dots, m,$$

where  $B_\tau$  incorporates the variability in the prediction error, making it adaptive to the observed data. This ensures that the Kalman filter remains robust even under conditions where the underlying system dynamics exhibit significant variability. The recursive process starts with the initial values  $\widetilde{y}_{1|0} = E\{y_1\}$  and  $L_{1|0} = \text{Var}(y_1)$ , which establish the initial state of the filter.

To estimate the unknown parameters  $\underline{\theta}$ , the quasi-log-likelihood function  $\log \mathcal{L}(\underline{z}; \underline{\theta})$  is maximized. Given the intricate nature of the model, explicit analytical expressions for the estimates at the point of maximization are typically unavailable. Consequently, advanced numerical optimization techniques are essential for accurately identifying the optimal parameter set that best reflects the observed data. These methods rely on iterative procedures that systematically explore the parameter space and converge toward values that maximize the likelihood function, yielding robust and consistent parameter estimates that capture the model's underlying stochastic dynamics. Furthermore, particle algorithms serve as powerful tools in approximating these quantities, leveraging the algorithm's output to achieve this goal. For instance, Ghezal and Alzeley [18] introduced a comprehensive framework involving a filtering algorithm (particle filter algorithm) designed to generate filtered particles and a smoothing algorithm (particle smoothing algorithm) to refine the estimates. These algorithms significantly improve the accuracy of the parameter estimation process, particularly in scenarios where traditional methods may struggle due to the model's nonlinearity and complexity.

**Remark 3.1.** *The recursive nature of parameter estimation in the logTG-SV model hinges on a well-structured innovation-update mechanism integrated into the quasi-maximum likelihood framework. The estimation process begins with initializing the predictor  $\widetilde{y}_{1|0}$  and its associated mean square error  $L_{1|0}$ . At each step  $\tau$ , the model dynamically updates the predicted value using asymmetric coefficients  $b_1$  and  $b_2$  depending on the sign of  $\Delta_{\tau-1}$ , calculates the innovation variance  $B_\tau$ , and incorporates the*



observed discrepancy between actual and predicted log-squared returns to update  $\Delta_\tau$ . This is followed by the update of the error variance via the auxiliary process  $A_\tau$ , ensuring adaptive tracking of volatility dynamics. This recursive system provides a computationally efficient path for likelihood approximation without resorting to full optimization over the entire sample.

In terms of estimation methodology, the sequential Monte Carlo (SMC) approach, particularly the particle filtering algorithm, is favored over conventional Bayesian techniques such as Markov chain Monte Carlo (MCMC). Meanwhile, MCMC methods, including Griddy-Gibbs sampling, are capable of approximating the posterior distribution of latent variables, but they often suffer from slow convergence and inefficiencies in high-dimensional or non-Gaussian environments. In contrast, the particle filter provides a nonparametric and flexible framework that updates in real time, handles nonlinearity effectively, and does not require closed-form transition densities. As demonstrated in Ghezal and Alzeley [18], SMC methods achieve robust performance and numerical stability, making them especially suitable for models like  $\log TG - SV$  that combine latent stochastic volatility with asymmetric responses to market shocks.

#### 4. Monte Carlo simulations

To evaluate the performance of the  $\log TG - SV$  model in accurately estimating its parameters, a series of Monte Carlo simulations was conducted. The simulations were designed to investigate how different sample sizes impact the precision of the parameter estimates. Three distinct sample sizes,  $m = 1000$ ,  $m = 2000$ , and  $m = 5000$ , were chosen for this purpose. For each sample size, a total of 500 independent replications were performed. The estimation results are summarized in Table 1, which reports the estimated parameters alongside their true values, with standard deviations shown in parentheses. These results provide valuable insights into the model's performance across different sample sizes, highlighting the robustness and reliability of the estimation procedure.

**Table 1.** Monte Carlo analysis of parameter estimation in the  $\log TG - SV$  model.

Parameters	Tv	$m = 1000$	$m = 2000$	$m = 5000$	95% CI (5000)
$a$	2.000	2.0396 (0.0762)	1.9692 (0.0548)	1.9784 (0.0271)	[1.9253, 2.0315]
$b_1$	0.065	0.0577 (0.0523)	0.0595 (0.0378)	0.0638 (0.0162)	[0.0321, 0.0955]
$b_2$	0.015	0.0135 (0.0484)	0.0131 (0.0401)	0.0141 (0.0089)	[-0.0033, 0.0315]
$c$	0.200	0.1830 (0.0547)	0.1891 (0.0312)	0.1978 (0.0109)	[0.1765, 0.2191]
$d$	0.100	0.0865 (0.0932)	0.0904 (0.0161)	0.0939 (0.0051)	[0.0840, 0.1038]

The Monte Carlo simulations conducted to evaluate the performance of the  $\log TG - SV$  model in parameter estimation reveal a clear trend of increasing accuracy as the sample size grows. Specifically, for parameter  $a$ , the estimates progressively approach the true value 2.000 as the sample size increases, with the smallest standard deviation observed at  $m = 5000$ , indicating enhanced precision. Similarly, the estimates for  $b_1$  and  $b_2$  demonstrate closer alignment with their true values as the sample size increases, with significantly reduced standard deviations, underscoring the model's robustness in handling larger datasets. Parameters  $c$  and  $d$  show a consistent pattern of higher accuracy and lower variability with increasing sample sizes, further reinforcing the model's reliability. To provide a more comprehensive statistical interpretation of the results, 95% confidence intervals have been reported

for the estimates at  $m = 5000$ . These intervals offer a formal measure of estimation uncertainty and validate whether the observed deviations from true values are statistically meaningful. Importantly, all true parameter values lie within their corresponding confidence bounds, confirming that the estimation procedure yields unbiased and statistically reliable results. This further demonstrates the model's capacity to deliver accurate and stable parameter estimates, particularly when larger sample sizes are utilized, thereby highlighting its robustness in capturing the data's underlying dynamics.

## 5. Modeling fluctuations in the algerian Dinar-Euro exchange rate using $\log TG-SV$ models

In the study of financial markets, exchange rates play a crucial role in understanding economic stability and predicting future market trends. The fluctuations in the Algerian Dinar-Euro exchange rate present a complex dynamic requiring sophisticated modeling to accurately capture the underlying patterns. The  $\log TG-SV$  model, known for its ability to model stochastic volatility with a threshold effect, provides a robust framework for analyzing these fluctuations. To facilitate the analysis, we first transform the original price series into logarithmic returns, which are defined as  $\lambda_\tau = \log\left(\frac{P_\tau}{P_{\tau-1}}\right)$ , where  $P_\tau$  and  $P_{\tau-1}$  denote the current and previous prices, respectively. This transformation stabilizes the variance, allows for easier interpretation of percentage changes, and aligns with the modeling assumptions of stationarity in volatility models. This section applies the  $\log TG-SV$  model to the Algerian Dinar-Euro exchange rate data covering the period from January 3, 2000, to September 29, 2011, as previously studied by Alzeley and Ghezal [32]. The analysis begins with an in-depth exploration of the descriptive statistics for both the raw exchange rate and the derived return series. These statistics are summarized in Table 2 below:

**Table 2.** Descriptive statistics for exchange rate series and logarithmic returns.

The series	Mean	SD	Median	Max	Min	Skew	Kurt	JB
Exchange rate	88.611	11.575	91.099	109.069	67.203	-0.518	2.132	$2.32 \times 10^2$
Log returns	0.00011	0.0050	0.0001	0.0496	-0.0233	0.3535	8.9678	$45.97 \times 10^2$
Absolute log returns	0.00357	0.0035	0.002554	0.049695	0.00000	2.6956	18.430	$340.08 \times 10^2$
Squared log returns	0.00002	0.00007	0.000007	0.002470	0.00000	16.1026	464.369	$272.27 \times 10^5$

Table 2 presents the descriptive statistics for the Algerian Dinar-Euro exchange rate and its transformed series: log returns, absolute log returns, and squared log returns. The exchange rate series has a mean of 88.611 with a standard deviation of 11.575, indicating moderate variability. The negative skewness (-0.518) implies a slight tendency towards lower exchange rates, while the kurtosis value (2.132) is close to that of a normal distribution. However, the Jarque-Bera (JB) test statistic ( $2.32 \times 10^2$ ) indicates potential deviations from normality. The log returns show a mean close to zero, reflecting the typical behavior of financial returns, where daily fluctuations average out over time. However, its high kurtosis (8.9678) and elevated JB statistic ( $45.97 \times 10^2$ ) indicate a leptokurtic distribution, implying a greater likelihood of extreme values, a common feature in financial data. The absolute and squared log returns further highlight this behavior, with the squared log returns displaying extremely high kurtosis (464.369), signaling strong volatility clustering. This pattern reflects the empirical regularity observed in financial markets, where periods of intense volatility are often followed by relatively calm phases. Next, we analyze the correlations of log returns at different lags, as shown in Table 3:

**Table 3.** Correlations of log returns at different lags.

Lag	1	2	3	4	5	6	7	8	9	10
$\widehat{corr}(\lambda_\tau, \lambda_{\tau-h})$	0.0357	0.0109	0.0124	0.0147	0.0360	0.0266	0.0209	0.0245	0.0065	-0.0070

Table 3 presents the autocorrelations of the log returns ( $\lambda_\tau$ ) with their past values at various lags (1 to 10). The results indicate a relatively weak but noticeable autocorrelation structure, with the first and fifth lags showing the highest correlations of 0.0357 and 0.0360, respectively. The presence of non-zero autocorrelations at specific lags implies that past returns exert some influence on future returns, consistent with typical financial time series behavior, where short-term dependencies are common. This autocorrelation pattern is essential for understanding the memory effects in exchange rate dynamics and further supports the use of the *logTG-SV* model in capturing such dependencies. Furthermore, we examine the time series of daily price returns in Figure 1:

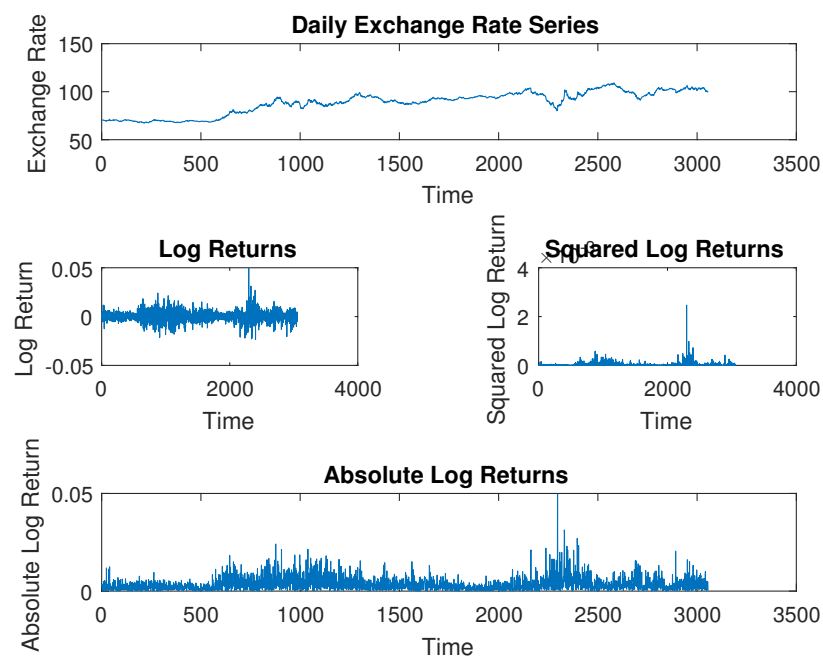
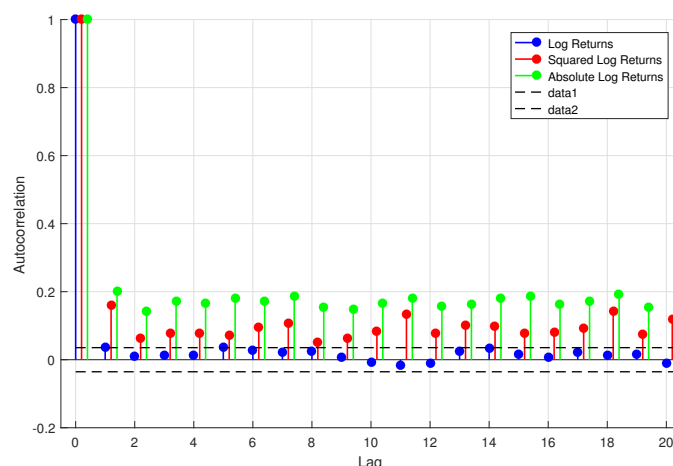
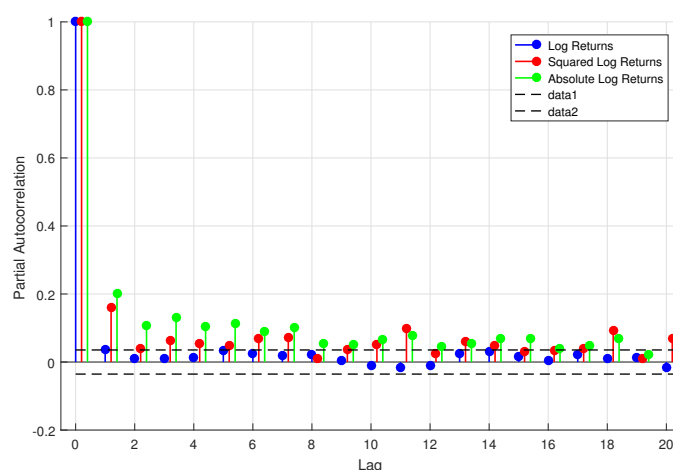
**Figure 1.** Time series of daily price returns, squared returns, and absolute returns.

Figure 1 displays the time series of daily price returns, showcasing log returns, squared log returns, and absolute log returns. The log returns fluctuate around a mean close to zero, reflecting typical daily market volatility. This pattern indicates that the market experiences both positive and negative price changes with no significant long-term drift. The squared and absolute log returns highlight periods of heightened volatility, which appear as clusters. This clustering effect, often referred to as volatility clustering, is common in financial markets, where periods of high volatility tend to follow each other, leading to sharp peaks in these plots. These observations align with the expected behavior of financial time series, where volatility is not constant over time but instead varies, often in response to market events. Next, we present the autocorrelation function of the log returns, squared log returns, and absolute log returns in Figure 2:



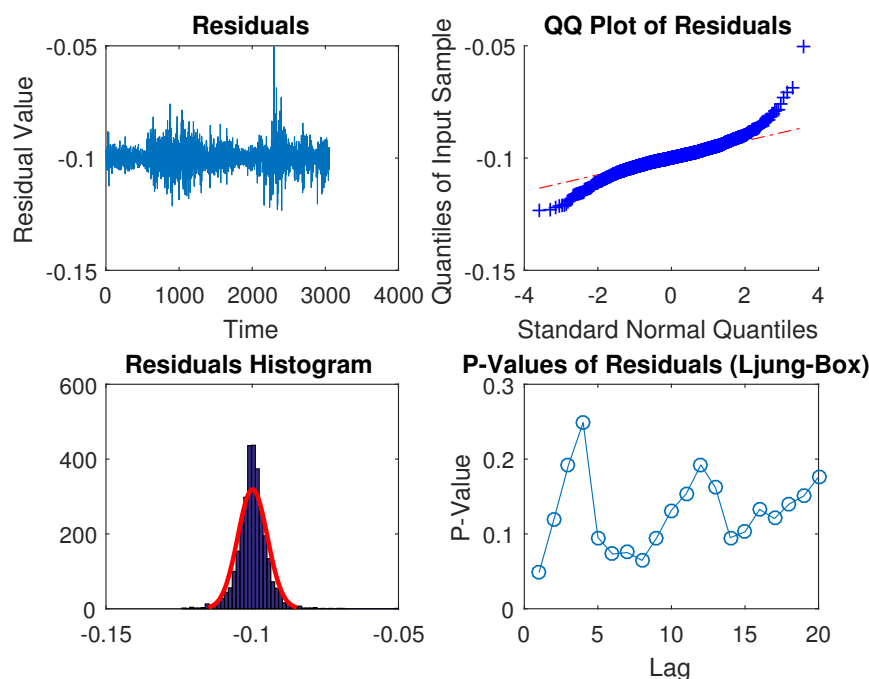
**Figure 2.** Autocorrelation function of log returns, squared returns, and absolute returns.

Figure 2 displays the autocorrelation functions ( $ACF$ ) for the log returns, squared log returns, and absolute log returns of the Algerian Dinar-Euro exchange rate series. The  $ACF$  of the log returns fluctuates around zero, with low values across the initial lags, indicating a weak autocorrelation structure. This behavior aligns with the efficient market hypothesis, which posits that returns in well-functioning markets exhibit minimal serial dependence. In contrast, the  $ACF$ s of the squared and absolute log returns show significant positive autocorrelations, especially at the first few lags. This pattern suggests the presence of volatility clustering, a common feature in financial time series, where periods of high (or low) volatility tend to be followed by similar periods. The slow decay in autocorrelation values for squared and absolute returns confirms that the volatility is not randomly distributed over time, but instead exhibits persistence. This justifies the use of the  $logTG-SV$  model, which is specifically designed to capture such dynamics in conditional heteroskedasticity. Following the analysis of autocorrelation, we illustrate the partial autocorrelation function in Figure 3:



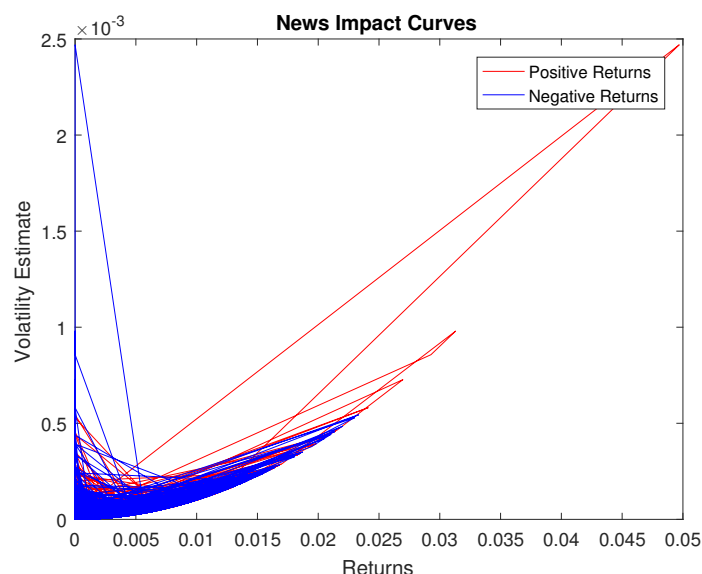
**Figure 3.** Partial autocorrelation function of log returns, squared returns, and absolute returns.

Figure 3 illustrates the partial autocorrelation functions (*PACF*) corresponding to the same return transformations. The *PACF* of the log returns exhibits a significant spike at lag 1, followed by rapid decline, indicating that most of the information about the current return is contained in the immediate past value. This confirms that the log return series follows a short-memory process. On the other hand, the *PACF*s of the squared and absolute log returns show significant values not only at lag 1, but also at higher-order lags, though the intensity diminishes progressively. This finding supports the presence of long-memory behavior in the volatility process, reinforcing the earlier *ACF* observations. The ability of the *PACF* to isolate the direct influence of specific lags further emphasizes the suitability of the *logTG-SV* model in modeling the conditional variance structure, particularly due to its capacity to incorporate threshold effects and capture persistent nonlinear dependencies in the volatility dynamics. Next, we turn to the analysis of the residuals of the model in Figure 4:



**Figure 4.** Residual analysis: Time series plot, QQ plot, and histogram.

Figure 4 focuses on the residuals of the time series model applied in the analysis. The residuals are plotted over time, showing fluctuations around zero, which indicates that the model captures the general trend of the data fairly well. However, the QQ plot comparing the residuals to a normal distribution reveals deviations, particularly in the tails, suggesting that the residuals are not perfectly normally distributed. This could imply the presence of outliers or periods where the model does not fully account for the observed variability. The histogram of the residuals further supports this, showing a distribution that deviates from normality, which may point to the need for model refinement or the consideration of alternative modeling approaches that better capture the underlying data dynamics. Finally, we examine the news impact curves presented in Figure 5:



**Figure 5.** News impact curves: The effect of positive and negative returns on market volatility.

Figure 5 presents the news impact curves, illustrating the relationship between the sign of returns (positive or negative) and the subsequent volatility in the market. The curves demonstrate that negative returns generally lead to a more significant increase in volatility compared to positive returns. This asymmetry suggests that the market reacts more strongly to negative news, which is a well-documented phenomenon in financial markets. The increased volatility following negative returns reflects heightened uncertainty and risk perception among investors during adverse market conditions, leading to more substantial price adjustments as the market processes and reacts to the new information. To further assess the comparative effectiveness of the proposed *logTG-SV* model, we estimated and contrasted the model parameters across three frameworks, *logTG-SV*, *TSV*, and *GARCH*, based on their respective in-sample volatilities. The table below summarizes the estimated values alongside their *RMS Es* to evaluate accuracy and robustness.

**Table 4.** Estimated parameters and *RMS Es* of in-sample volatility across *logTG-SV*, *TSV*, and *GARCH* models.

Parameters	<i>log TG-SV</i>	model	<i>TSV</i>	model	<i>GARCH</i>	model
$a$	-0.0143	(0.0018)	-0.0316	(0.0045)	0.0965	(0.0189)
$b_1$	0.7682	(0.0159)	0.8586	(0.0258)	0.9479	(0.0342)
$b_2$	0.0393	(0.0136)	0.0672	(0.0304)	—	—
$c$	0.4023	(0.0602)	0.5064	(0.0758)	0.5487	(0.0861)
$d$	0.7012	(0.0452)	0.7197	(0.0495)	—	—

The results in Table 4 provide a comprehensive evaluation of model robustness and estimation precision. For parameter  $a$ , which reflects the volatility intercept, the *logTG-SV* model achieves the smallest RMSE (0.0018), indicating the highest estimation accuracy compared to *TSV* and *GARCH* counterparts. Regarding the persistence parameters  $b_1$  and  $b_2$ , the *logTG-SV* model again demonstrates

lower RMSEs, highlighting its capacity to more reliably capture the memory structure of volatility. Similarly, the parameters  $c$  and  $d$  also show reduced estimation errors under the  $\log TG-SV$  model. This indicates a stronger ability to capture nonlinear features commonly observed in financial return series. Overall, the inclusion of both stochastic volatility and threshold effects in the  $\log TG-SV$  structure leads to more accurate and stable parameter estimation. These findings reinforce the model's superiority in characterizing the volatility dynamics of the Algerian Dinar-Euro exchange rate.

## 6. Conclusions

This study introduces the  $\log TG-SV$  model as a novel extension of traditional stochastic volatility frameworks by integrating two core innovations: a logarithmic transformation of past volatility shocks and an asymmetric threshold mechanism that distinguishes between the effects of positive and negative returns. This hybrid structure enables the model to capture both volatility clustering and asymmetric shock responses, stylized facts commonly observed in financial markets but often insufficiently addressed by classical SV or GARCH-type structures. From a theoretical perspective, we derived sufficient conditions to ensure both strict and second-order stationarity of the model, as well as the existence of its higher-order moments. These conditions guarantee that the  $\log TG-SV$  process is statistically well-posed and appropriate for reliable inference and long-term forecasting. Empirically, the Monte Carlo simulations provided compelling evidence of the model's estimation stability and accuracy. For varying sample sizes ( $m = 1000, 2000, \text{ and } 5000$ ), the estimated parameters consistently approached their true values with decreasing standard deviations. In the real-data application, we modeled the daily fluctuations of the Algerian Dinar-Euro exchange rate over a span of more than a decade. The analysis revealed the typical features of financial time series: excess kurtosis, volatility clustering, and asymmetric response to shocks. The  $\log TG-SV$  model effectively captured these empirical features. The news impact curve (Figure 5), in particular, confirmed that negative shocks induce larger volatility responses than positive ones, which is in line with the model's design and the observed market asymmetry. The residual diagnostics further supported the model's validity, showing residuals centered around zero and partial autocorrelation structures confirming short- memory behavior. Although some deviations from normality remained in the residuals, these can motivate future extensions incorporating heavy-tailed or skewed innovation distributions.

In conclusion, the  $\log TG-SV$  model represents a notable advancement in stochastic volatility modeling, effectively integrating log-volatility dynamics with threshold asymmetry. It exhibits robust theoretical properties, strong finite-sample estimation capabilities, and practical effectiveness in capturing the intricate dynamics of exchange rate behavior. Future research could adapt the model to multivariate settings, include regime changes, or use it for high-frequency financial data.

## Use of Generative-AI tools declaration

The author declares he has not used Artificial Intelligence (AI) tools in the creation of this article.

## Conflict of interest

The author declares no conflicts of interest in this paper.

## References

1. T. Bollerslev, Generalized autoregressive conditional heteroskedasticity, *J. Econometrics*, **31** (1986), 307–327. [https://doi.org/10.1016/0304-4076\(86\)90063-1](https://doi.org/10.1016/0304-4076(86)90063-1)
2. D. B. Nelson, Conditional heteroskedasticity in asset returns: A new approach, *Econometrica*, **59** (1991), 347–370. <https://doi.org/10.2307/2938260>
3. R. Engle, GARCH 101: The use of ARCH/GARCH models in applied econometrics, *J. Econ. Perspect.*, **15** (2001), 157–168. <https://doi.org/10.1257/jep.15.4.157>
4. S. J. Taylor, Financial returns modelled by the product of two stochastic processes: A study of the daily sugar prices 1961–1979, In: *Time series analysis: theory and practice I*, Amsterdam:North-Holland, 1982, 203–226.
5. F. Black, Noise, *J. Financ.*, **41** (1986), 528–543. <https://doi.org/10.1111/j.1540-6261.1986.tb04513.x>
6. E. Jacquier, N. G. Polson, P. E. Rossi, Bayesian analysis of stochastic volatility models with fat-tails and correlation errors, *J. Econometrics*, **122** (2004), 185–212. <https://doi.org/10.1016/j.jeconom.2003.09.001>
7. A. Ghezal, I. Zemmouri, On the Markov-switching autoregressive stochastic volatility processes, *SeMA*, **81** (2024), 413–427. <https://doi.org/10.1007/s40324-023-00329-1>
8. Z. X. Ding, C. W. J. Granger, R. F. Engle, A long memory property of stock market returns and a new model, *J. Empir. Financ.*, **1** (1993), 83–106. [https://doi.org/10.1016/0927-5398\(93\)90006-D](https://doi.org/10.1016/0927-5398(93)90006-D)
9. A. C. Harvey, Long memory in stochastic volatility, In: *Forecasting volatility in the financial markets*, 3 Eds., Oxford: Butterworth-Heinemann, 2007, 351–363. <https://doi.org/10.1016/B978-075066942-9.50018-2>
10. M. A. Carnero, D. Peña, E. Ruiz, Persistence and kurtosis in *GARCH* and stochastic volatility models, *J. Financ. Economet.*, **2** (2004), 319–342. <https://doi.org/10.1093/jjfinec/nbh012>
11. J. Yu, On leverage in a stochastic volatility model, *J. Econometrics*, **127** (2005), 165–178. <https://doi.org/10.1016/j.jeconom.2004.08.002>
12. C.-J. Kim, C. R. Nelson, State-space models with regime switching: classical and Gibbs-sampling approaches with applications, *J. Am. Stat. Assoc.*, **95** (2003), 1373–1374. <https://doi.org/10.2307/2669796>
13. A. Melino, S. M. Turnbull, Pricing foreign currency options with stochastic volatility, *J. Econometrics*, **45** (1990), 239–265. [https://doi.org/10.1016/0304-4076\(90\)90100-8](https://doi.org/10.1016/0304-4076(90)90100-8)
14. S. Chib, F. Nardari, N. Shephard, Markov chain Monte Carlo methods for stochastic volatility models, *J. Econometrics*, **108** (2002), 281–316. [https://doi.org/10.1016/S0304-4076\(01\)00137-3](https://doi.org/10.1016/S0304-4076(01)00137-3)
15. A. Doucet, S. Godsill, C. Andrieu, On sequential Monte Carlo sampling methods for Bayesian filtering, *Stat. Comput.*, **10** (2000), 197–208. <https://doi.org/10.1023/A:1008935410038>
16. J. Danielson, Stochastic volatility in asset prices: estimation with simulated maximum likelihood, *J. Econometrics*, **64** (1994), 375–400. [https://doi.org/10.1016/0304-4076\(94\)90070-1](https://doi.org/10.1016/0304-4076(94)90070-1)



17. F. J. Breidt, A threshold autoregressive stochastic volatility model, *VI Latin American Congress of Probability and Mathematical Statistics (CLAPEM)*, Valparaiso, Chile, 1996.
18. A. Ghezal, O. Alzeley, Probabilistic properties and estimation methods for periodic threshold autoregressive stochastic volatility, *AIMS Mathematics*, **9** (2024), 11805–11832. <https://doi.org/10.3934/math.2024578>
19. A. Ghezal, M. Balegh, I. Zemmouri, Markov-switching threshold stochastic volatility models with regime changes, *AIMS Mathematics*, **9** (2024), 3895–3910. <https://doi.org/10.3934/math.2024192>
20. H. Tong, On a threshold model, In: *Pattern recognit and signal processing*, Netherlands: Sijtho and Noordho, 1978, 575–586. [http://dx.doi.org/10.1007/978-94-009-9941-1\\_24](http://dx.doi.org/10.1007/978-94-009-9941-1_24)
21. M. K. P. So, W. K. Li, K. Lam, A threshold stochastic volatility model, *J. Forecasting*, **21** (2002), 473–500. <https://doi.org/10.1002/for.840>
22. C. W. S. Chen, F. C. Liu, M. K. P. So, Heavy-tailed-distributed threshold stochastic volatility models in financial time series, *Aust. N. Z. J. Stat.*, **50** (2008), 29–51. <https://doi.org/10.1111/j.1467-842X.2007.00498.x>
23. X. P. Mao, E. Ruiz, H. Veiga, Threshold stochastic volatility: properties and forecasting, *Int. J. Forecasting*, **33** (2017), 1105–1123. <https://doi.org/10.1016/j.ijforecast.2017.07.001>
24. J. Geweke, Modelling persistence in conditional variances: A comment, *Economet. Rev.*, **5** (1986), 57–61.
25. S. G. Pantula, Modeling the persistence of conditional variances: A comment, *Economet. Rev.*, **5** (1986), 71–74. <https://doi.org/10.1080/07474938608800099>
26. R. F. Engle, T. Bollerslev, Reply, *Economet. Rev.*, **5** (1986), 81–87. <https://doi.org/10.1080/07474938608800101>
27. C. Francq, G. Sucarrat, An exponential chi-squared *QMLE* for *log-GARCH* models via the *ARMA* representation, *J. Financ. Economet.*, **16** (2018), 129–154. <https://doi.org/10.1093/jjfinec/nbx032>
28. G. Sucarrat, The *log-GARCH* model via *ARMA* representations, In: *Financial mathematics, volatility and covariance modelling*, London: Routledge, 2019, 336–359.
29. G. Sucarrat, A. Escribano, Estimation of *log-GARCH* models in the presence of zero returns, *Eur. J. Financ.*, **24** (2018), 809–827. <https://doi.org/10.1080/1351847X.2017.1336452>
30. R. A. Davis, T. Mikosch, Probabilistic properties of stochastic volatility models, In: *Handbook of financial time series*, Berlin: Springer, 2009, 255–267. [https://doi.org/10.1007/978-3-540-71297-8\\_11](https://doi.org/10.1007/978-3-540-71297-8_11)
31. A. Doucet, A. M. Johansen, A tutorial on particle filtering and smoothing: fifteen years later, In: *The Oxford handbook of nonlinear filtering*, Oxford: Oxford University Press, 2011, 656–705.
32. O. Alzeley, A. Ghezal, On an asymmetric multivariate stochastic difference volatility: structure and estimation, *AIMS Mathematics*, **9** (2024), 18528–18552. <http://doi.org/10.3934/math.2024902>